Properties of Semipolar InGaN QWs Grown on 3D Inverse GaN Pyramids

Thomas Wunderer

The properties of thin InGaN films deposited via MOVPE on non-planar GaN surfaces are investigated in detail. Using a comprehensive combination of different investigation methods including transmission electron microscopy, spatially and time-resolved cathodoluminescence experiments and modeling of the radiative recombination kinetics a precise description of the semipolar QW properties can be presented.

1. Introduction

Today's commercially available GaN based light emitting devices are limited in their efficiency. High piezoelectric fields hamper the radiative recombination of carriers within the QWs. The fields result from the biaxially strained InGaN films and the polar character of the hexagonal wurtzite crystal structure. Together, they cause a local separation of electron and hole wave functions and consequently less efficient device structures [1, 2]. This fact is most prominent for high In-compositions which are needed for longer wavelength emitters. Less polar crystal orientations, wherefore a higher recombination probability is expected [3, 4], could be one way to overcome the so-called 'green gap'.

That is why many groups are currently dealing with the properties of non- and semipolar group III-nitrides [5, 6]. Today, the most convincing way to fabricate high performance non- and semipolar GaN devices is to use GaN substrates with high material quality. They can be obtained from quasi-GaN-boules with a thickness of a view millimeters which are typically grown in the conventional c-direction and then prepared for the desired crystal orientation [7]. The substrates typically feature a very low defect density which seems to be the key factor for the remarkable device performance on such substrates [6]. However, the high prize and the small sample size are limiting factors for commercial applications [8]. An interesting alternative approach for semipolar device structures is the usage of three-dimensional (3D) GaN and naturally formed semipolar side facets. We could demonstrate that high material quality can be achieved using inverse GaN pyramids at low fabrication costs on large substrate sizes [9].

In this work the properties of thin InGaN films which have been deposited onto the 3D surfaces are investigated. The specific geometry of the underlying structure influences the growth behavior during the deposition process via metal-organic vapor phase epitaxy (MOVPE).

2. Fabrication Procedure

The epitaxial growth was performed by low pressure MOVPE in an Aixtron single wafer reactor. First, high quality GaN templates with a thickness of about 2 µm were grown on c-plane sapphire wafers. The optimized fabrication procedure includes the deposition of a SiN interlayer for efficient defect reduction [10]. Then, a 200 nm thick SiO_2 layer was deposited via plasma enhanced chemical vapor deposition (PECVD). Optical lithography and dry etching techniques were subsequently applied for structuring the SiO_2 mask into hexagonal patterns. Afterwards, the samples have been taken back into the MOVPE reactor to grow the 3D structures. Thereon, we have grown the InGaN QWs. In order to get an appropriate In incorporation, the QWs as well as the GaN barriers in between were grown at a reduced temperature of about 800 °C, whereas all other layers have been typically grown in the temperature range of $T = 950$–1050°C

3. InGaN Properties

The structural properties of an InGaN/GaN MQW stack deposited on 3D GaN are strongly influenced by the specific geometry of the underlying structure [11]. Different to planar growth, the structured surface may affect the thicknesses as well as the composition of the ternary InGaN films which directly influence the optical properties of the structure. A particularly strong variation of the QW emission wavelength was found on a relatively large inverse GaN pyramids with 13 µm long $\{11\bar{2}2\}$ side facets. Spatially resolved cathodoluminescence investigations showed an enormous shift of the wavelength from about 530 nm at the top of the structure towards 380 nm at the inner tip of the inverse pyramid (Fig. 1).

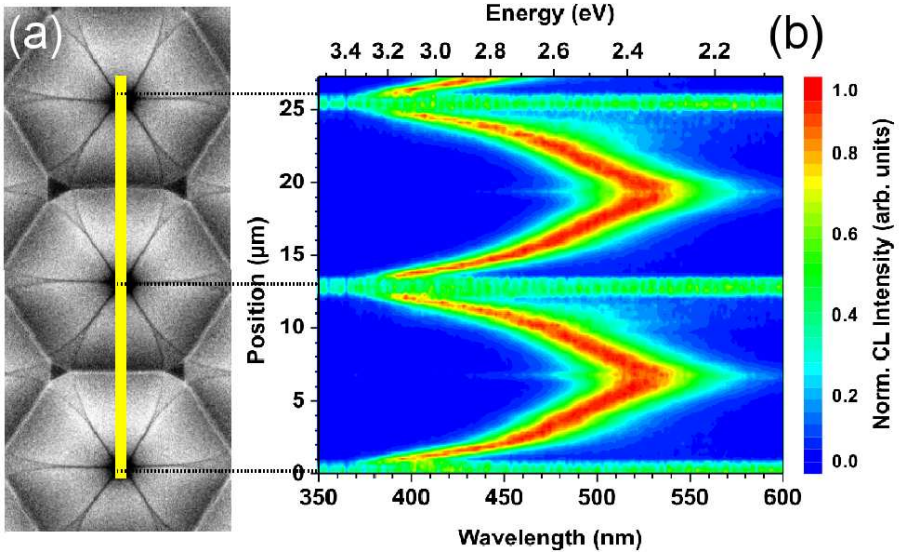

Fig. 1: SEM top view of inverse pyramid structure with $\{11\bar{2}2\}$ facets and a period length of 13 µm (a) and respective CL wavelength linescan (b). The data was acquired by S. Metzner, Otto-von-Guericke-Universität Magdeburg.

The emission wavelength of an InGaN QW is dependent on various parameters. The most prominent factors are the indium composition, the QW thickness and the piezoelectric field which changes the transition energy within the QW due to the quantum confined Stark effect (QCSE). All parameters are strongly correlated and, therefore, can not be treated isolated. We have been able to build a comprehensive picture of the QW properties by combining the structural and optical properties with theoretical model calculations.

First, the QW thickness was determined along the complete facet length using transmission electron microscopy (TEM). A small lamella was prepared using focused ion beam (FIB) techniques to cut the desired specimen perpendicular to the facet surface. The determined QW thickness from the TEM images along the facet is shown in Fig. 2.

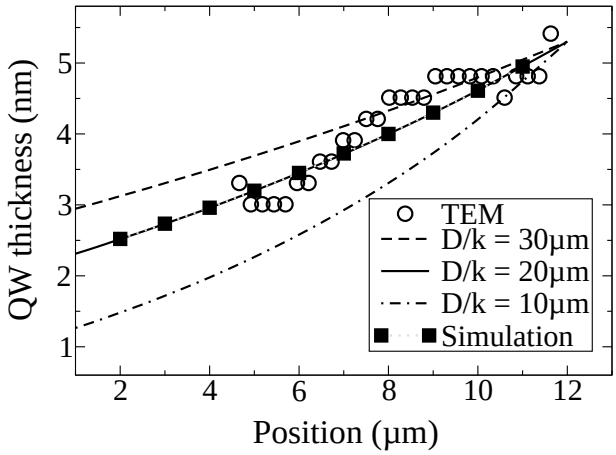

Fig. 2: QW thickness along inverse pyramid facet. Position 0 corresponds to the inner tip.

It was found that gas phase diffusion processes in selective area growth (SAG) can precisely describe the growth behavior using MOVPE [12]. We confirmed that the QW thicknesses on 3D GaN with only one facet type can also be well modeled by gas phase diffusion (not shown). That is the reason why we applied the gas phase diffusion model to our problem taking into account the specific geometry of the 3D structure. For simplicity, we first used a constant InGaN composition to determine the QW thickness which should be sufficiently accurate due to the low indium concentration. As shown in Fig. 2, the best matching was found for $D/k = 20\,\mu\text{m}$ for the film, where D is the diffusion coefficient and k is the rate constant for the first-order heterogeneous surface adsorption and can be understood as a value for the actual incorporation of the respective species [13, 14].

To fully describe the QW properties, two other parameters, the indium composition and the strength of the piezoelectric field, have to be quantized for any position along the facet. The values can be gained by including two additional independent measures - the transition energy and the radiative life time. Cathodoluminescence experiments can provide access to both of them. The spectral properties as well as the time-dependence of the radiation can be gained with the necessarily spatial accuracy. Figs. 3 and 4 show the transition energy and radiative life time of the QW emission for any position along the facet.

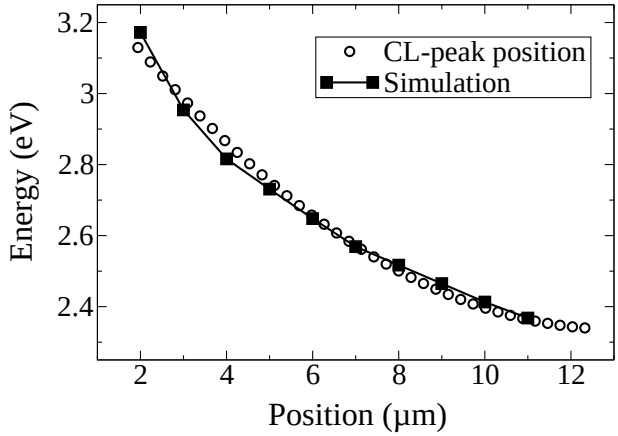

Fig. 3: QW transition energy along inverse pyramid facet. Position 0 corresponds to the inner tip.

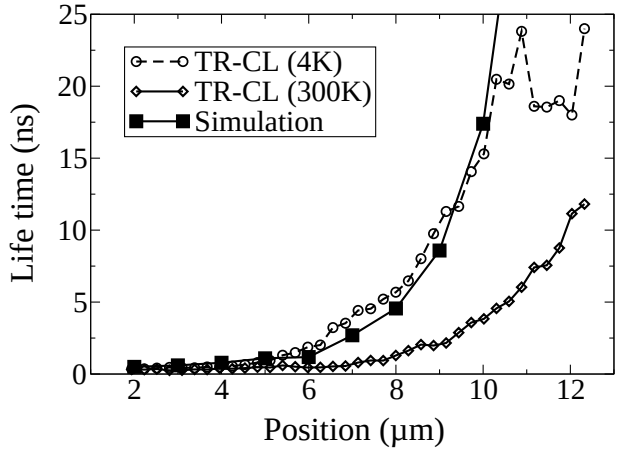

Fig. 4: Carrier life time along inverse pyramid facet. Position 0 corresponds to the inner tip.

As can be seen, the model calculations perfectly match the experimental data. The simulation is based on a fairly comprehensive model of the QW properties solving self-consistently the Schrödinger and Poisson equation for each individual point along the facet.

As a result, we now know the indium composition and the strength of the piezoelectric field for all data points along the facet (Fig. 5). A fairly constant indium composition of about 20 % is found on the upper half of the inverse pyramid and is then strongly decreasing towards the inner tip. This finding can be understood when looking closer to the growth conditions used to deposit the InGaN films. Typically, InGaN is grown under a high overdose of TMIn. Despite a smaller D/k for indium (here: $D/k = 5\,\mu\mathrm{m}$), the oversupply of TMIn is still present for the upper half of the pyramid and, therefore, the composition within the solid is mainly determined by the growth rate of the film and not by the gas composition. This is different in the lower half of the pyramid. Here, actually the gas composition determines the composition in the solid as the oversupply of indium is not valid any more (not shown).

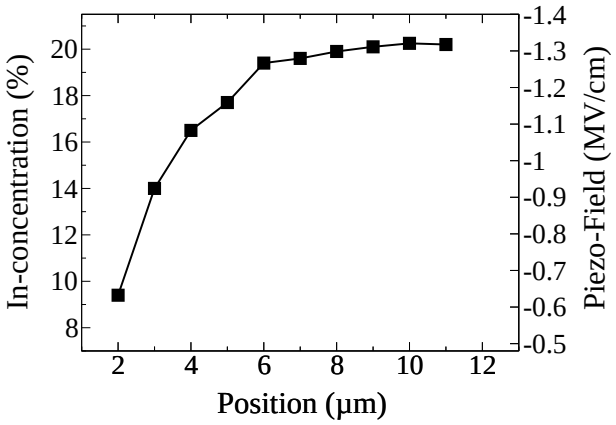

Fig. 5: In-composition along inverse pyramid facet. Position 0 corresponds to the inner tip.

For the piezoelectric tensor elements, we have found the best matching to the experimental data using the values from the most recent publications [15, 16]. This leads to a piezoelectric field of about -1.3 MV/cm^2 for an In-composition of 20 % on the semipolar $\{11\bar{2}2\}$ plane. This is about 1/3 of the value found for QWs grown on c-plane GaN.

Interestingly, the structure is well suited to determine the piezoelectric field without knowledge of the piezoelectric constants or exact indium composition. Bulashevich et al. developed an analytical approach to determine the piezoelectric polarization by varying the QW thickness [17]. Due to the QCSE the change in QW thickness directly converts into a shift of the emission wavelength. Using our inverse pyramid structure, we have access to an accurate variation of the QW thickness originating from gas phase diffusion. Furthermore, we have shown that a nearly constant In-content can be assumed in the upper half of the facet. This structure therefore is ideally suited for the determination of the piezoelectric field using Bulashevich's model:

$$E_{e,h} - E^0_{e,h} = -\frac{512 m_{e,h} e^2 F^2 d^4}{243 \pi^6 \hbar^2 \chi^2} \tag{1}$$

with $E^0_{e,h}$ as the ground state for electrons and holes without electrical field F:

$$E^0_{e,h} = \frac{\pi^2 \hbar^2}{2 m_{e,h} d^2} \tag{2}$$

Hereby, e and h represents electrons and holes, χ is the screening of the field by carriers. Due to the low excitation we can set $\chi = 1$ in our case. The thickness of the QWs is given by d. Fig. 6 shows the measured emission energy via CL and the respective model calculations for different values of the piezoelectric field. The best matching has been achieved for a piezoelectric field of about 1-1.3 MV/cm. This value can be gained without the knowledge of the exact In-composition and piezoelectric constants. However, assuming about 20 % indium in the QWs (see above) the value fits very well to the findings from Shen et al. [18].

Finally, the determined data set is used to estimate the internal quantum efficiency (IQE) at different positions of the structure. Assuming that at low temperature (4 K) the carrier

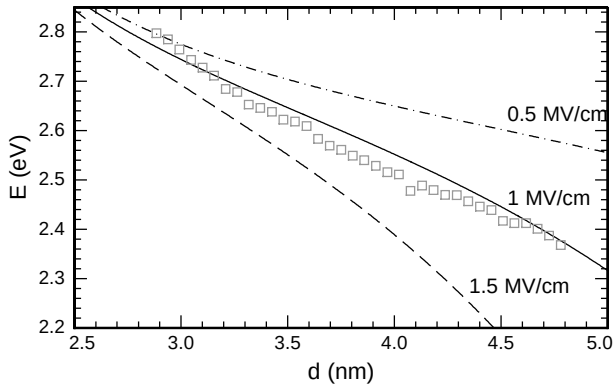

Fig. 6: CL emission energy along upper half of inverse pyramid in correlation with determined QW thickness (squares) (section 4). Shift of emission energy for different field strengths using the analytic model of Bulashevich et al. [17]. Curves are normalized.

recombination is mainly driven by radiative recombination processes, an upper value for the IQE can be given:

$$\eta_{IQE}(300\,\mathrm{K}) = \frac{\tau(300\,\mathrm{K})}{\tau_\mathrm{r}(300\,\mathrm{K})} \leq \frac{\tau(300\,\mathrm{K})}{\tau_\mathrm{r}(4\,\mathrm{K})} \leq \frac{\tau(300\,\mathrm{K})}{\tau(4\,\mathrm{K})} \tag{3}$$

The life times along the facet (Fig. 4) were combined with the emission wavelength at the specific position (Fig. 3). The following diagram for the IQE vs. wavelength can than be created (Fig. 7). The diagram shows the typical drop of the IQE towards longer wavelength emission which is known as the green gap. Although the piezoelectric polarization could be reduced by about 2/3 in comparison to c-plane devices, the fields are still quite strong for high indium compositions. Additionally, it is assumed that point defects at the interfaces of the QWs play a significant role as non-radiative recombination channels which are generated during the low temperature growth of the QWs. Together, they limit the overall efficiency, especially in the green wavelength regime.

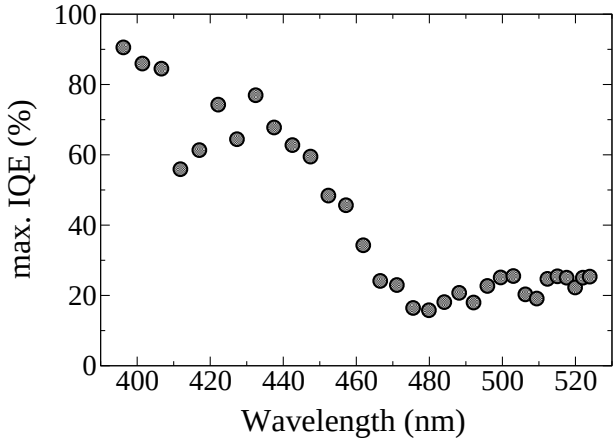

Fig. 7: Max. IQE vs wavelength determined using Equ. 3 and the carrier life times from Fig. 4.

4. Conclusion

A detailed study of InGaN QWs deposited on semipolar $\{11\bar{2}2\}$ side facets of inverse pyramids is presented. A comprehensive combination of different investigation methods including TEM, spatially and time-resolved CL experiments and modeling of the radiative recombination process allow the exact determination of QW thickness, indium composition and piezoelectric polarization. Furthermore the data set is used to estimate an IQE for different wavelength. Despite a significant reduction of the piezoelectric field, the 'green gap' is still present.

Acknowledgement

We gratefully acknowledge the fruitful cooperation with M. Feneberg and S. Metzner (Otto-von-Guericke-Universität Magdeburg) for the model calculations and CL investigations, respectively. L. Lechner and J. Biskupek (Ulm University) performed great work for the TEM investigations.

References

[1] J.S. Im, H. Kollmer, J. Off, A. Sohmer, F. Scholz, and A. Hangleiter, "Reduction of oscillator strength due to piezoelectric fields in GaN/$Al_xGa_{1-x}N$ quantum wells", *Phys. Rev. B*, vol. 57, pp. R9435–R9438, 1998.

[2] A. Hangleiter, J. Im, H. Kollmer, S. Heppel, J. Off, and F. Scholz, "The role of piezoelectric fields in GaN-based quantum wells", *MRS Internet J. Nitride Semicond. Res.*, vol. 3, p. 15, 1998.

[3] T. Takeuchi, S. Sota, M. Katsuragawa, M. Komori, H. Takeuchi, H. Amano, and I. Akasaki, "Quantum-confined stark effect due to piezoelectric fields in GaInN strained quantum wells", *Jpn. J. Appl. Phys.*, vol. 36, pp. L382–L385, 1997.

[4] T. Takeuchi, H. Amano, and I. Akasaki, "Theoretical study of orientation dependence of piezoelectric effects in wurtzite strained GaInN/GaN heterostructures and quantum wells", *Jpn. J. Appl. Phys.*, vol. 39, pp. 413–416, 2000.

[5] T. Paskova, *Nitrides with Nonpolar Surfaces*. Weinheim: Wiley-VCH, 2008.

[6] J.S. Speck and S.F. Chichibu, Guest Editors, "Nonpolar and semipolar group III nitride-based materials", *MRS Bulletin*, vol. 34, pp. 304–309, 2009, Special issue containing several articles authored by various groups.

[7] K. Fujito, S. Kubo, and I. Fujimura, "Development of bulk GaN crystals and nonpolar/semipolar substrates by HVPE", *MRS Bulletin*, vol. 34, pp. 313–317, 2009.

[8] U. Schwarz and M. Kneissl, "Nitride emitters go nonpolar", *phys. stat. sol. (RRL)*, vol. 1, pp. A44–A46, 2007.

[9] T. Wunderer, J. Wang, F. Lipski, S. Schwaiger, A. Chuvilin, U. Kaiser, S. Metzner, F. Bertram, J. Christen, S.S. Shirokov, A.E. Yunovich, and F. Scholz, "Semipolar GaInN/GaN light-emitting diodes grown on honeycomb patterned substrates", *phys. stat. sol. (c)*, vol. 7, pp. 2140–2143, 2010.

[10] J. Hertkorn, F. Lipski, P. Brückner, T. Wunderer, S. Thapa, F. Scholz, A. Chuvilin, U. Kaiser, M. Beer, and J. Zweck, "Process optimization for the effective reduction of threading dislocations in MOVPE grown GaN using in situ deposited SiN_x masks", *J. Cryst. Growth*, vol. 310, pp. 4867–4870, 2008.

[11] W. Feng, V.V. Kuryatkov, A. Chandolu, D.Y. Song, M. Pandikunta, S.A. Nikishin, and M. Holtz, "Green light emission from InGaN multiple quantum wells grown on GaN pyramidal stripes using selective area epitaxy", *J. Appl. Phys.*, vol. 104, pp. 103530-1–4, 2008.

[12] D. Ottenwälder, "Untersuchungen zur selektiven Epitaxie im Halbleitersystem GaIn(As,P)", Dissertation, Physikalisches Institut der Universität Stuttgart, 1996.

[13] H. Fang, Z.J. Yang, Y. Wang, T. Dai, L.W. Sang, L.B. Zhao, T.J. Yu, and G.Y. Zhang, "Analysis of mass transport mechanism in InGaN epitaxy on ridge shaped selective area growth GaN by metal organic chemical vapor deposition", *J. Appl. Phys.*, vol. 103, pp. 014908-1–4, 2008.

[14] S. Keller, B.P. Keller, D. Kapolnek, A.C. Abare, H. Masui, L.A. Coldren, U.K. Mishra, and S.P.D. Baars, "Growth and characterization of bulk InGaN films and quantum wells", *Appl. Phys. Lett.*, vol. 68, pp. 3147–3149, 1996.

[15] H. Shen, M. Wraback, H. Zhong, A. Tyagi, S.P. DenBaars, S. Nakamura, and J.S. Speck, "Determination of polarization field in a semipolar $(11\overline{2}2)$ InGaN/GaN single quantum well using Franz–Keldysh oscillations in electroreflectance", *Appl. Phys. Lett.*, vol. 94, pp. 241906-1–3, 2009.

[16] M. Feneberg, K. Thonke, T. Wunderer, F. Lipski, and F. Scholz, "Piezoelectric polarization of semipolar and polar GaInN quantum wells grown on strained GaN templates", *J. Appl. Phys.*, vol. 107, pp. 103517-1–6, 2010.

[17] K.A. Bulashevich, S.Y. Karpov, and R.A. Suris, "Analytical model for the quantum-confined Stark effect including electric field screening by non-equilibrium carriers", *phys. stat. sol. (b)*, vol. 243, pp. 1625–1629, 2006.

[18] H. Shen, M. Wraback, H. Zhong, A. Tyagi, S.P. DenBaars, S. Nakamura, and J.S. Speck, "Unambiguous evidence of the existence of polarization field crossover in a semipolar InGaN/GaN single quantum well", *Appl. Phys. Lett.*, vol. 95, pp. 033503-1–3, 2009.